THIS ARTICLE IS UNDER FORMATTING AS THE PDF IS READY, FILE WILL BE REPLACED

Effect of Nano-Additives on the Emissions, Performance, and Combustion Characteristics of Syzygium cumini (Jamun) Biodiesel Powered DI Engine

R.Anbazhagan[*1], P.Naveenchandran[2]

[1*]*Research Scholar, Department of Automobile Engineering, Bharath Institute of Higher Education and Research, Chennai, Tamil Nadu, India*

[2] *Professor, Department of Automobile Engineering, Bharath Institute of Higher Education and Research, Chennai, Tamil Nadu, India*

*****Corresponding author: **anbu.mit@gmail.com**

Abstract

Renewable and cleaner diesel engine fuel has received a lot of attention recently as a result of the depletion of fossil resources. To address this issue, biodiesel can be a potential substitute for diesel fuel. The finest B20 Jamun blends were combined with three different types of nanoadditives to create Syzygium cumini (Jamun) biodiesel, which was tested in a naturally aspirated diesel engine. Global researchers are starting to develop new nanoadditives in the meantime, which is an authoritative and efficient method. This technology was combined with different biodiesels. Also included in this chapter is an examination of a test engine using three distinct nano-additives: titanium dioxide (TiO_2), zirconium oxide (ZrO_2), and cerium oxide (CeO_2). These additives were combined to create the best blends of Syzygium cumini (B20), and the results were evaluated based on factors such as performance, combustion, and output emissions. Additionally, a proposal is made to further improve the construction of a realistic and economically feasible nanoparticle addition for diesel and biodiesel fuel.

Keywords: ***performance, Combustion, Emission, Biodiesel, Additives***

1. Introduction

Increasing fuel prices and the depletion of fossil fuels have caused the demand for biofuels to grow in commercial and industrial engines. The modern world could benefit from the use of biodiesel as a sustainable energy source [1]. As a clean-burning fuel, biodiesel aids in reducing emissions of smoke, carbon monoxide (CO), and unburned hydrocarbons (HC) [2]. On the other hand, decreased brake power (BP) and greater brake-specific fuel consumption (BSFC) are noted as a result of lower heating values compared to petroleum-based fuels [3]. Nitrogen oxide (NOx) emissions are also said to rise with the use of biodiesel [4]. Researchers investigated the effects of several oxygenated additives on biofuels in order to improve combustion and emission characteristics. Thermal efficiency and heat release rates were commonly boosted by metallic oxide nanoparticles [5].

In essence, the additives made of nanoparticles act as catalysts. Their high surface-to-volume ratio makes them more reactive, which accelerates the rate at which fuel burns [6]. Among the most often used nanoadditives are cerium oxide, aluminium oxide, cobalt oxide, and zinc oxide because of their special makeup, which helps to burn fuel within engine cylinders more efficiently [7]. It's critical that the nanoparticles in the fuel mixture be well mixed. Studies have shown that using an ultrasonic fuel blender and surfactant can help create a single-phase nanoparticle fuel blend. In a study by Balu P et al., silica nano-additives were added (at 50, 75, and 100 ppm) to 20% maize oil methyl ester blends with diesel [8]. According to test results, adding nano-additives helped to reduce HC emissions by encouraging full combustion and providing enough oxygen at higher loads by functioning as an oxygen buffer. A higher evaporation rate and higher oxidation property of the fuel result from nano-additives, which promote full combustion. They also found decreased smoke emissions for mixed fuels with nano-additives. Cymbopogonflexuosus biofuel (CFB) was examined for combustion, performance, and tailpipe emissions using a CI engine by Balu P et al. (2016) [10]. For the C20-D80 blend, it was deduced that employing CFB lowers the BTE by 6% and 9%, respectively, at half and full load. Additionally, it was found that while the EGT significantly rose, the CFB and its mixes decreased peak pressure, ignition delay, and HRR. It led to a decrease in the range of CO_2, smoke opacity, hydrocarbon, and NOx emissions and increased CO_2 emissions during peak load [11]. This study investigates the performance, combustion, and emission characteristics of a single-cylinder diesel engine using a variety of nanoparticle Syzygium cumini (Jamun) biodiesel fuel blends.

2. Three Different Nanoadditives are characterised

To assess the shape and nature of the titanium, zirconium, and cerium nanoadditives, SEMs were used. It was used in conjunction with grain production and minor agglomeration to determine the crystal nature. Figure 1 displays the SEM morphology of these three nanoadditives. Using a 30 kV applied voltage and a VEGA3 TESCAN model, SEM characterization was carried out. In order to study this sample, a thin plate coated in gold was placed in a 0.01 Torr vacuum environment to create the specimen's surface contact. The SEM image result showed that the particles were uniformly dispersed and aggregated throughout the sample. The nanoadditives exhibit differences in diameter and surface vacancy growth upon stimulation by the sol-gel method. These three nanoadditives' TEM morphology study was examined using the JEM-3010 ultrahigh-resolution analytic electron microscope, as shown in Figure 1. It is evident that every particle was evenly spaced across the crystal.

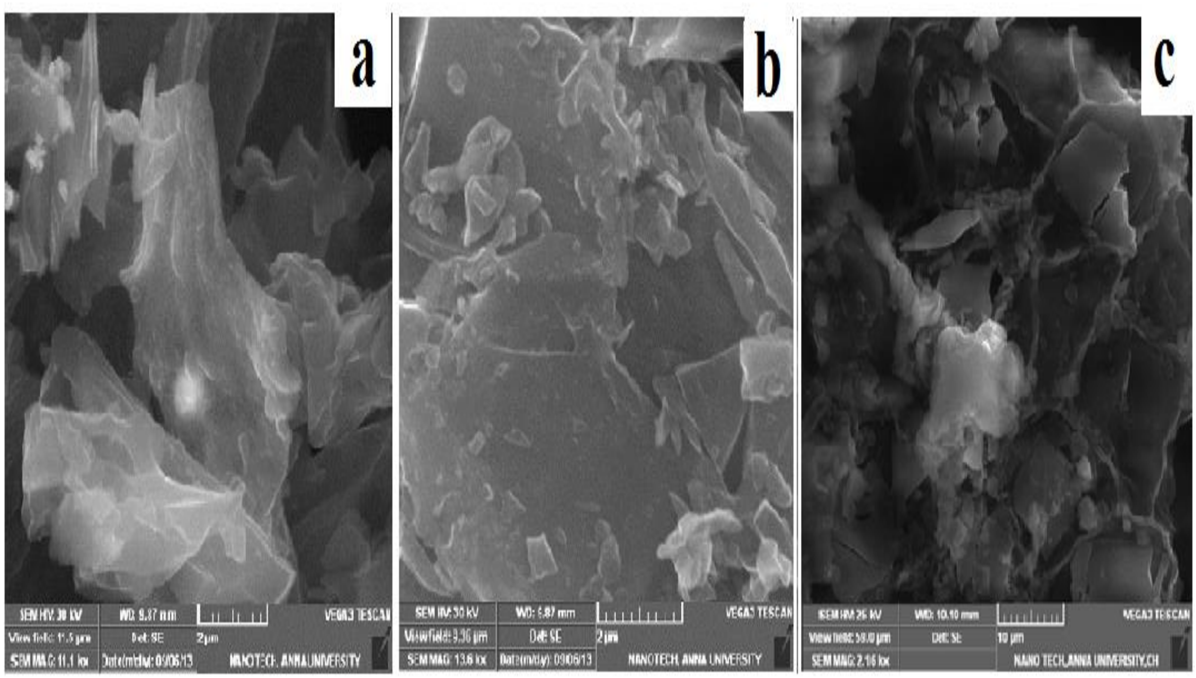

Figure 1. SEM morphological image of (a) cerium nanoadditive (b) titanium nanoadditive and (c) zirconia nanoadditive

Table 3.1. Nanofuels effects on fuel properties of SEME - Syzygium Cumini (Methyl Esters) and its blends

Test fuel properties	Units	ASTM D6751	Diesel	Syzygium cumini	B20	B20+ ZrO_2	B20+ CeO_2	B20+ TiO_2
Density @ 15ºC	g/cm^3	0.858	0.831	0.886	0.837	0.841	0.843	0.84
Viscosity @ 40ºC	mm^2/s	1.9-6.0	3.2	5.14	3.9	4.1	4.2	4
Flash Point	ºC	Min.130	70	181	86	92	93	91
Cetane Number	-	Min.47	46	57	50	52	54	53
Higher heating value	MJ/kg	-	43.82	39.88	42.12	41.1	40.78	41.92

3. Test Engine Setup

At first, an eddy current dynamometer with a dynamometer and electrical resistance was attached to an air-cooled test engine. It was tested with 5.2 kW of power at a steady speed of 1500 rpm. In order to monitor the pressure rise versus crank angle on a flywheel, a Kistler-made piezoelectric pressure transducer, model number 7063-A, was mounted to the test engine and coupled to a crank angle encoder [9]. The engine was installed alongside the SES combustion analyzer. The input signal from the diesel engine was the primary use for the encoder, analyzer, and charge amplifier manufactured by Kistler Instrument AG in Switzerland. Five gas analyzers were used to measure the buildup of tailpipe emissions, especially the emissions of HC, CO, CO_2, and NOx. The AVL 437 C smoke opacimeter was used to measure the smoke opacity emission from the QROTECH Co. Ltd. and QRO 402 type Korean-made instrument. Figure 2 describes the Kirloskar DI diesel engine arrangement. For this engine test, SAE 40 lubricating oil was used to increase engine performance and prevent wear and tear issues [19].

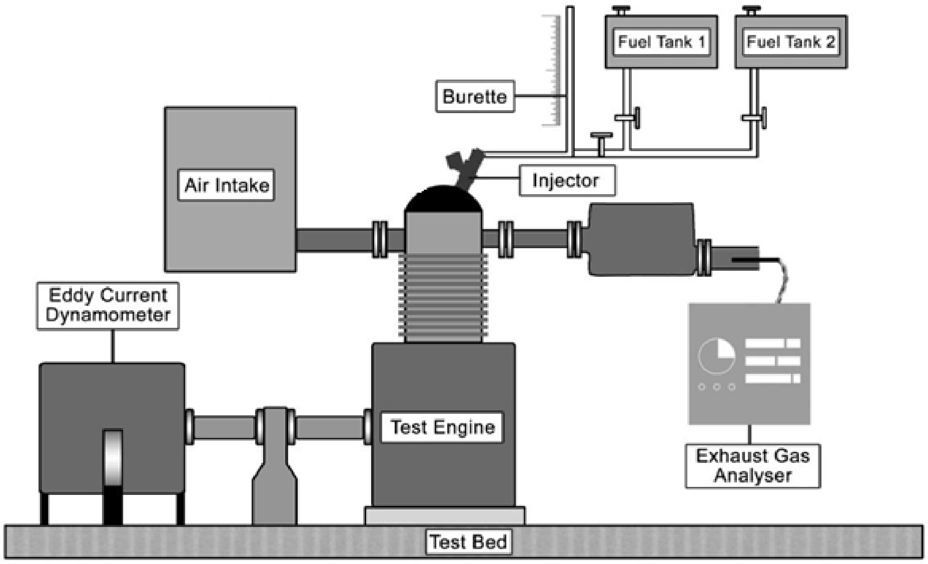

Figure 2 Engine set up

Table 1 Detailed Kirloskar makes diesel engine specification

Type	Four strokes, Direct Injection diesel engine
Make	Kirloskar TAF – 1
Bore and Cooling type	87.5 mm and air-cooled engine
Stroke	112 mm
Compression ratio	17.5:1
Rated power and speed	5.2kW at 1500 rpm
Injection timing	23 deg before Top Dead Center (static)
Number of nozzles and spray hole diameter	3 and 0.3 mm

Piston geometry	Hemispherical
Swept volume	661 cc

4. Results and Discussion

4.1 Brake Thermal Efficiency

Figure 3 shows the variations of BTE (%) vs. BP for blended nano-additives and Syzygium cumini (Jamun) blends. Figure 3 shows that the presence of different nanoadditives reduces the ignition delay and combustion time of biodiesel blends in diesel engines, which raises in-cylinder pressure, HRR levels, and correspondingly, BTE levels. The BTE of each Jamun blend was gradually raised with increasing load circumstances for the whole range of load situations. When compared to other fuel mixes, Jamun nano additive mixed fuel punches small and substantial fluctuations among them up to 100% engine load situations. At maximum load, blends with nanoadditives predominate, including Jamun B20 and B100 blends. The B20+TiO_2 (25 ppm) mix has 31.21% more BTE than other blends with nanoadditives and Jamun blends that are more similar to mineral diesel. Additionally, as compared to petroleum diesel, blended fuels containing B20+CeO_2 (25 ppm) and B20+ZrO_2 (25 ppm) had consecutive BTE values. This incident was attributed to the characteristics of titanium nanoparticles, which, due to their large thermal energy nature and superior fuel atomization rate, acted as an O_2 buffer to boost the burning zone during the combustion stage. Additionally, the fuel hydrocarbon is additionally crashed by the nanoadditives due to their catalytic cracking activity. The increased BTE trend is connected with the Jamun B20+TiO_2 (25 ppm) mix when compared to blended fuels with nano additives. This is caused by the presence of nanoscale compounds that prevent carbon from depositing during the combustion process [15].

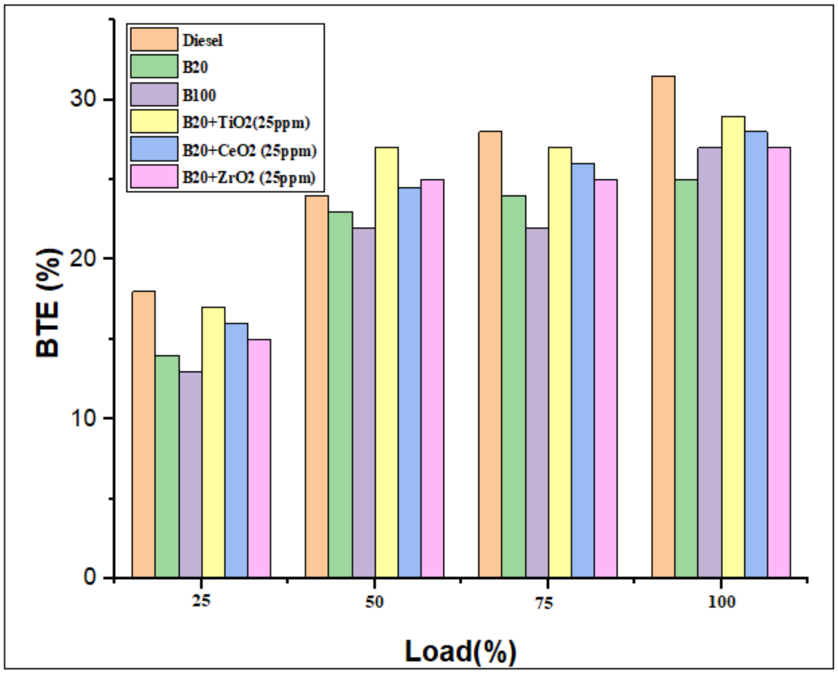

Figure 3. Brake thermal efficiency Vs Load

4.2 Specific fuel energy consumption

Figure 4 illustrates the gross augmentation of petroleum-diesel blends, B20, B100, and Jamun nanoadditives for BSEC against BP. For all fuel combinations, there was a slight drop in the value of BSEC due to the increased fuel concentration that occurs with higher engine loads. According to the BSEC trend, the combined impact of a larger viscosity range and minimum fuel calorific value yield starved atomization classified the Jamun B100 blend as being in a higher position for all load scenarios. Simultaneously, the equally distributed other nanoadditives had a higher rate of energy consumption with the petroleum-diesel mix and Jamun B20+TiO_2 (25 ppm). This was caused by excess fuel that was available in the fuel plunger to reserve the engine speed. At the maximal load spectrum, the B20+TiO_2 (25 ppm) mix's BSEC differed somewhat from that of the petroleum-diesel blend. It was also dropped by 17.53% with the B100 blend, and the B20+TiO_2 (25 ppm) blend outperformed another nanoadditives combination [12]. Fuel nanoadditives, which have a higher surface-to-volume ratio, provide greater external energy transfer, and serve as an oxygen source for burning, may be the cause of this. In a similar vein, the combination of these findings resulted in a decrease in engine friction and a correspondingly smaller range of BSEC for the B20+TiO_2 (25 ppm) mix [14].

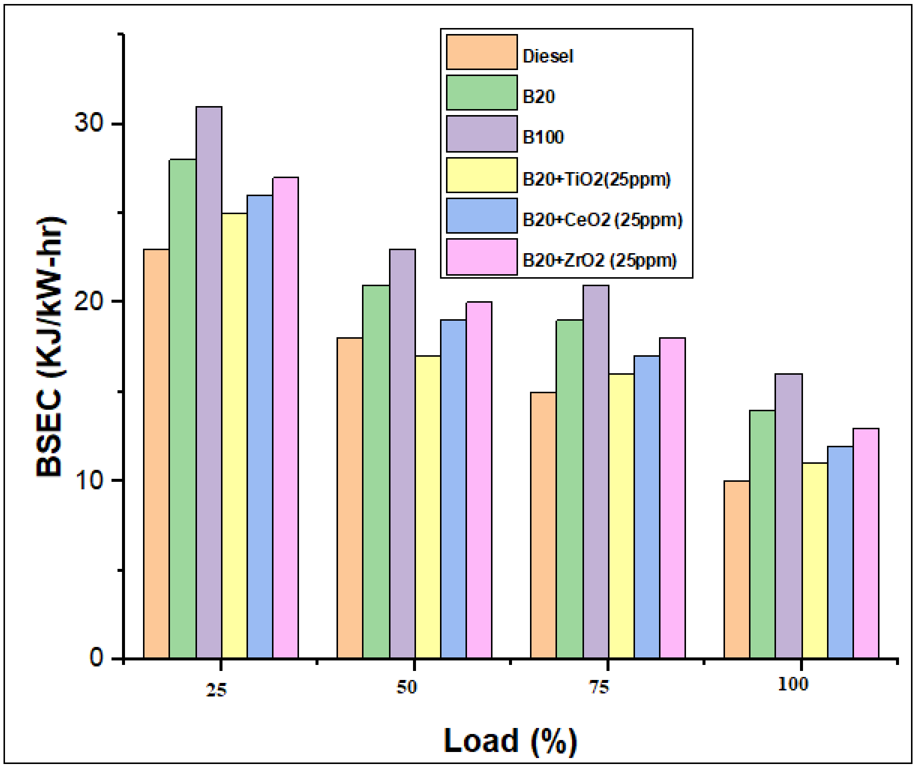

Figure 4. Specific fuel energy consumption Vs Load

4.3 CO Emission

The substantial variation in CO emissions for the whole Jamun, nanoadditives, and petroleum-diesel mixes in comparison to BP is shown in Figure 5. The plot shows that the CO emission range was consistently decreased up to 75% of load conditions, but at peak load, all fuel combination emissions abruptly surged throughout a wide range [15]. Mineral diesel produces a wider range of pollutants in this emission plot than other fuel mixes. Under full load conditions, raw B20 blends and nanoadditives+B20 blends exhibit a significant decline in value, which is correlated with petroleum-diesel. This decline is caused by the high surface-to-volume ratio of the nanoadditives, which allows for increased fuel atomization, increases the rate at which CO oxidises, influences the entire combustion state, and forms minimal CO emissions across the whole load spectrum. Due to the strong oxidising nature of the TiO_2 nanoparticles, the B20+TiO_2 (25 ppm) mix produces a

36.36% decreased CO emission range at greater loads, associated with petroleum-diesel fuel and somewhat lowered with other nanoadditives blends.

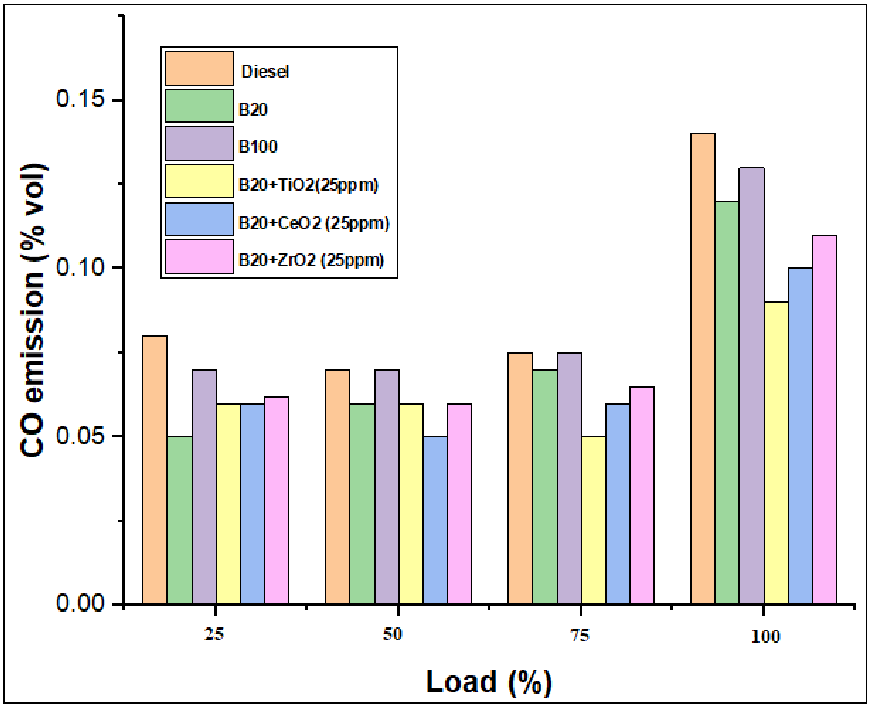

Figure 5. CO Emission Vs Load

4.4 UBHC emission

Figure 6 shows the variation of various fuel combinations with nanoadditives and jamun oil for UBHC against BP. The graph makes it evident that all fuel combinations' UBHC emissions rose at low load, fell at intermediate load, and abruptly climbed at high load [13]. The petroleum-diesel mixes progressively yield greater UBHC under all load circumstances. The plot clearly shows that the B20+TiO_2 (25 ppm) mix achieves a significant decrease in the fuel trend when combined with petroleum-diesel. Under full load conditions, the three nanoadditives' UBHC emission ratios decreased in a greater range when combined with petroleum-diesel (17.40%), B20+TiO_2 (25 ppm) (14.75), and B20+ZrO_2 (25 ppm) (16.57). O_2's usefulness, combined with the potential energy generated by nanoadditives, created this occurrence. When this event is integrated, the carbon deposit in the cylinder is burned off, and the remaining non-ionic chemicals are reduced. This significantly reduces fuel quenching, which leads to a significant decrease in fuel loss and facilitates the combustion process. The combustion process is influenced by this minimum activation temperature, and as a result, the UBHC emission was reduced more significantly [16].

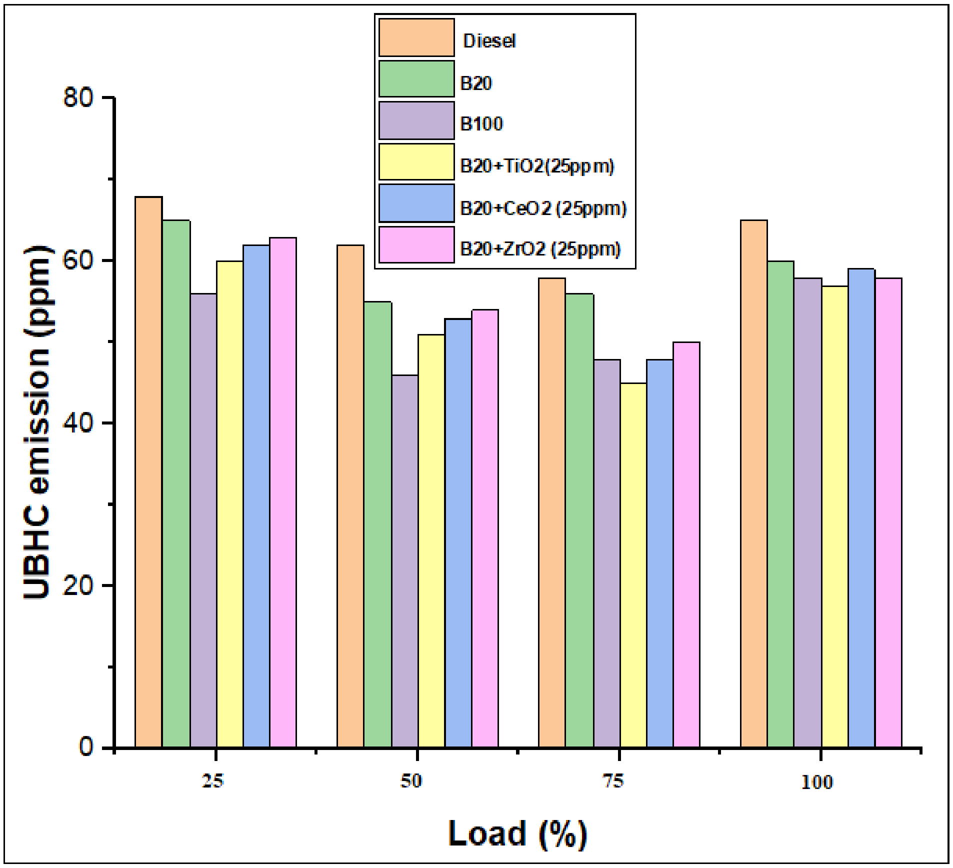

.

Figure 6. Unburnt hydrocarbon Vs Load

4.5 NOx Emission

Figure 7 displays the tested NOx emissions for all gasoline mixtures. The results of the NOx emission test indicate that the blends of mineral diesel, B20, and B20+nanoadditives are significantly different from the B100 blend [18]. Additionally, it was found that all of the test fuel combinations cause NOx emissions in the increasing load spectrum. The whole fuel mix should ideally establish the marginal level of emissions at 100% of the load, but during peak load circumstances, the NOx emission levels were much higher in parts per million as compared to earlier engine loads. The reason for this would be the reciprocal interaction between nitrogen and oxygen at high peak temperatures under full load. In comparison to other blends, mineral diesel exhibits reduced NOx emissions, indicating that petroleum-diesel fuel has a higher O_2 deficiency and a lower peak cylinder temperature. Because the fuel blend contains greater amounts of donating O_2, which helps to raise the cylinder temperature and reveal the source of increased NOx emission levels, the B20 blend performed better in terms of NOx emission during peak load when compared to nanomixed fuels. Ultimately, the greatest reduction in emission range with B100 blends is achieved by the B20+TiO_2 (25 ppm) fuel mix (22.57%). This was caused by the presence of nanometal oxides, which provide more oxygen concentration and more O_2 vacancies to support the oxidation of soot. By absorbing O_2 molecules during the combustion process, TiO_2 nanoparticles act as a reducing agent and increase the heat transfer range at low temperatures, which inhibits the generation of NOx. When compared to B20 blends with TiO_2, both B20+CeO_2 (25 ppm) and B20+ZrO_2 (25 ppm) blends reach higher emission levels. This is likely due to the insufficient combustion of test fuel droplets, which increases the formation of carbon on the walls of the combustion chamber. These events also raise the temperature, which leads to the formation of excess NOx.

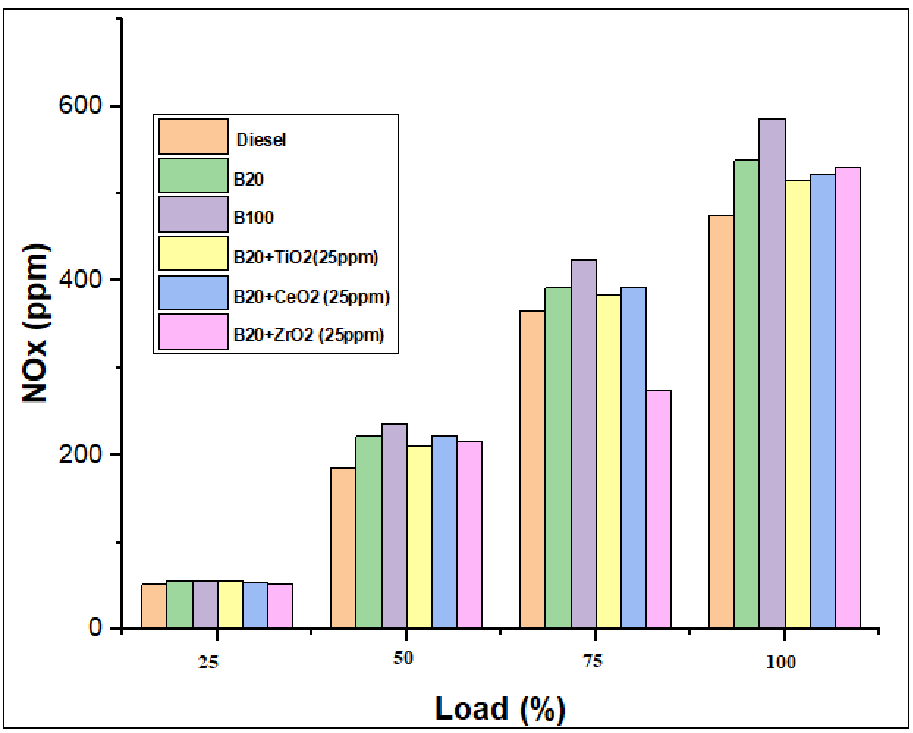

Figure 7 Oxides of nitrogen Vs Load

4.6 Smoke emission

The smoke emissions for all test gasoline mixes were sharply amplified under higher load circumstances, as shown in Figure 8. The smoke emissions of all fuel mixes do not significantly differ from one another at low engine loads; this may be attributed to lower fuel-rich areas, longer response times, and better diffusion combustion [17]. Compared to other fuel mixes, the smoke emissions from mineral diesel blends increased significantly. All of the nano-additives blended fuels resulted in reduced emission levels with petroleum-diesel blends at peak engine loads, but the B20+TiO_2 (25 ppm) mix offers 16.25% low smoke emission levels. The inclusion of a nanocomponent in the blend prevented this from happening by increasing the rate at which gasoline evaporates, reducing the amount of the "C" element in the exhaust, increasing the rate at which fuel and air combine, and improving ignition quality. In the meantime, diffusion combustion and the removal of the carbon content inside the walls were caused by the activation energy provided by the nanoadditives. Fuel blends with B20+TiO_2 (25 ppm) gradually reduce smoke emissions over the whole load range.

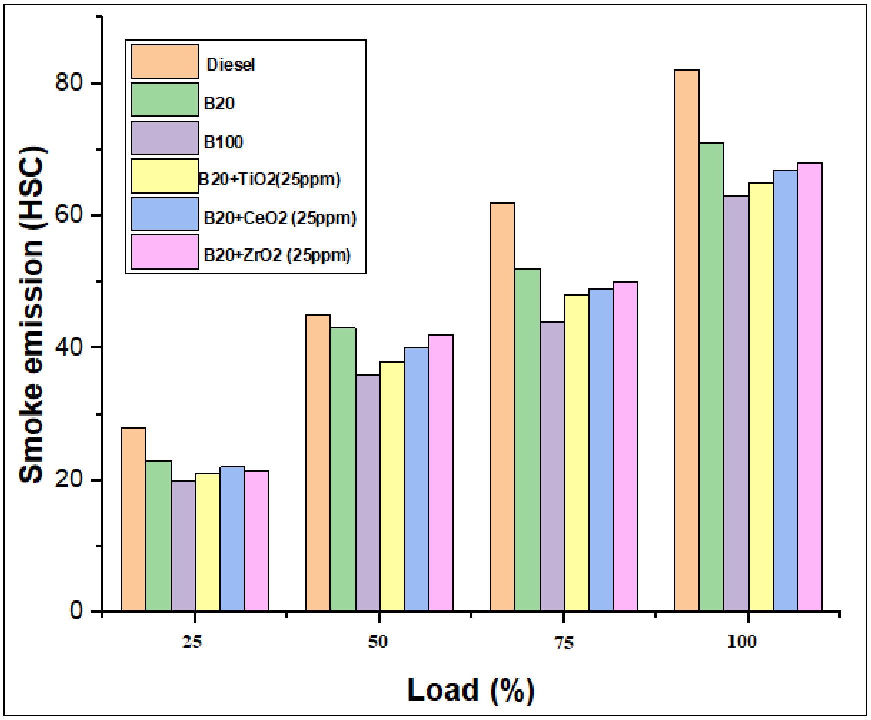

Figure 8. Smoke opacity Vs Load

4.7 Cylinder Pressure

Figure 9 illustrates how an ignorant range of pressure peaks is produced by all the pertinent fuel blend peaks. Higher and lower peaks are produced in that case by fuel mixes of mineral diesel (59.86 bar) and B100 (51.68 bar). The test fuels with nanoadditives then assign an increased peak pressure to the Jamun B20 mix. This means that the B20+TiO_2 (25 ppm) fuel blend produced a greater in-cylinder pressure of about 58.82 bar, which was somewhat closer to the petroleum-diesel peak than the B20+CeO_2 (25 ppm) fuel mix, which produced a lower peak pressure of 57.21 bar with both petroleum-diesel and B20+TiO_2 (25 ppm). The extra B20+ZrO_2 (25 ppm) blend was likewise found to have a pressure drop of 54.98 bar. This suggests that the B20 fuel blend should have a higher pressure of 54.48 bar than the B100 blend, which would be the rationale for a higher cetane number and the lowest possible test fuel viscosity. Additionally, the test fuel's O_2 molecules' ability to survive improves the cylinder combustion sequence. Due to the unique material characteristics of the TiO_2 nanoadditives mix, which increase the fuel dispersion range by increasing the surface-to-volume ratio of TiO_2, a higher-pressure peak of the blend was observed. Additionally, the O_2 vacancy is delivered by the atomic and cubic structures, and the nature of these nanoadditives results in a greater peak pressure. The fuel ID deviation, which results in an equal increase in premixed combustion phases.

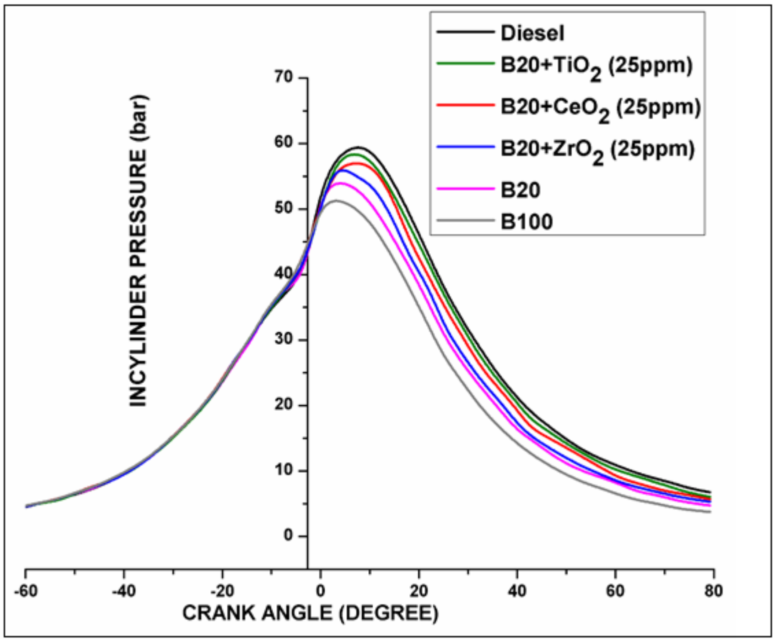

Figure 9. Cylinder pressure Vs Crank angle

4.8 Heat Release Rate

The variations of different fuel mixes with HRR profile vs. crank angle are displayed in Figure 10. The plot's negative HRR range may be caused by cooling effects and fuel vaporisation, which act to accelerate combustion and create a positive HRR range through a sharp rise in temperature. The figure indicates that the HRR range of mineral diesel was larger than that of the other fuel blends. This is because the mineral diesel retains minimal ignition delay with previous combustion, which maximises the HRR rate at premixed combustion rates as a result of a higher injection pressure rate. Because there are more oxygen molecules in the fuel than in the B100 mix, the Jamun B20 blend produces a higher HRR rate than the B100 blend. This expansion of combustion and peak in-cylinder pressure results in a higher HRR than the B100 blend. Then, when compared to the Jamun B20 blend, the blended fuels with nanoadditives had a higher HRR. The TiO_2 Jamun fuel blend also shows potential for future HRR enhancement because the nanoparticle acts as an O_2 source, transferring more O_2 molecules to the Jamun fuel blend during combustion, which may result in higher HRR. Furthermore, the TiO_2 nanoadditives developed more O_2 vacancies on their surfaces, which stimulated much lower activation energy. These properties resulted in the generation of greater oxygen mines for the future renovation of some fuel tailpipe emissions, namely CO and HC.

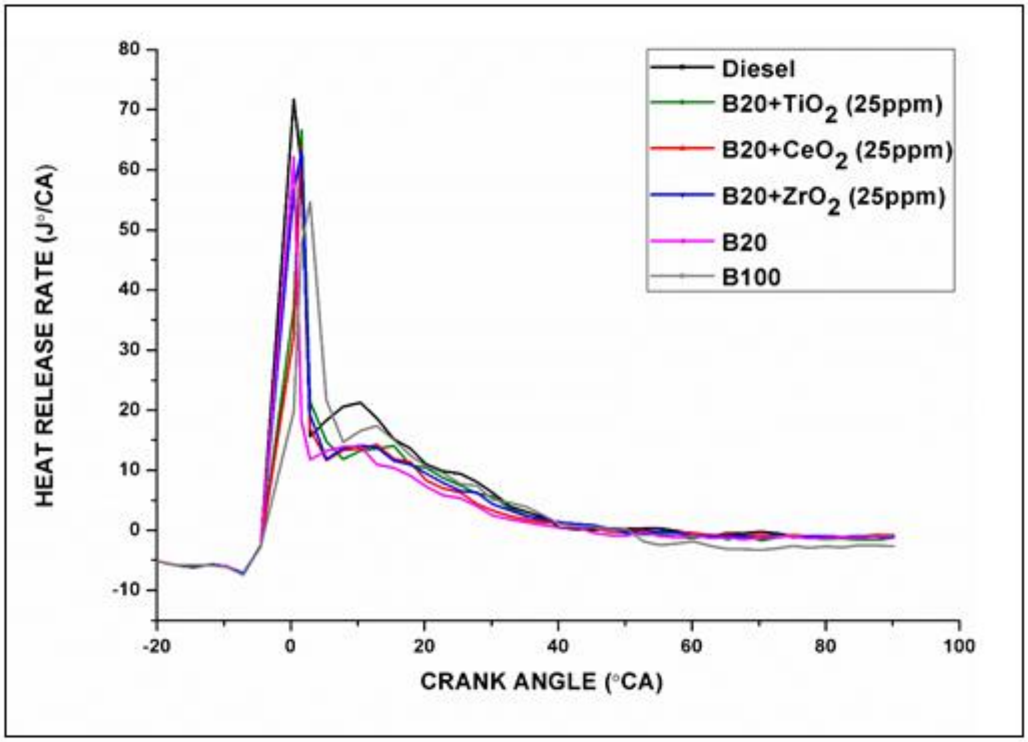

Figure 10. Heat Release Rate Vs Crank angle

5. Conclusion

Jamun biodiesel was chosen for this study's alternative feed stroke for DI diesel engines. According to the findings of its experimental testing, the Jamun B20 blend had a lower tailpipe emission range and was rated as having greater performance. However, the greatest B20 fuel blend was combined with unique, cutting-edge nanoadditives in this chapter, and it had to do with petroleum-diesel. The raw Jamun mixes under investigation produce higher emissions and lower performance levels. Novel nanoadditives were added to the gasoline mixes to boost performance levels and lower Jamun tailpipe emissions. The outcomes of the test engine's investigation were shown as follows:

- ❖ When compared to a B20 blend with an analogous range of petroleum-diesel, the B20+TiO_2 (25ppm) fuel mix has 6.05% greater BTE. However, the same blend has 10.67%

lower BSEC when compared to a Jamun B20 blend. Larger oxidation content, catalytic activity, and a larger surface to volume ratio of nano-additives made this possible.

- The B20+TiO_2 (25ppm) fuel mix resulted in decreased CO, UBHC, and smoke emissions when combined with mineral diesel, but greater NOx and CO_2 emissions.

- The B20+TiO_2 (25ppm) fuel blend's HRR and in-cylinder pressure reach a greater peak when compared to the B20 blend and the similar range with mineral diesel. This is because the nano additions' atomic and cubic structure provide the O_2 vacancy, which in turn leads to higher peak pressure and HRR.

- The use of nanoadditives in fuel blends results in a narrower range of viscosity and an improved fuel calorific value. This fuel feature enhances the performance levels of Jamun blends and demonstrates improved operation.

As can be seen from the above summary, the B20+TiO_2 (25ppm) blend was recommended as a cost-effective and integrated fuel for diesel engines. It also deserves a higher range of combustion and performance levels, as well as reduced tailpipe emissions when used with petroleum-diesel fuel.

Reference

[1]. Mukul T, Naveen K. Influence of nanoadditives on the performance and emission characteristics of a CI engine fuelled with diesel, biodiesel and blends – a review. Energy Sources, Part A: Recovery, Utilization, and Environmental Effects 2020; 42(23): 2944-61.

[2]. Chen AF, Akmal AM, Adam A, Othman FM, Kamal KM, Mrwan GA. Combustion characteristics, engine performances and emissions of a diesel engine using nanoparticle-diesel fuel blends with aluminium oxide, carbon nanotubes and silicon oxide. Energy Conversion and Management 2018; 171: 461–77.

[3]. Khalife E, Tabatabaei M, Demirbas A, Aghbashlo M. Impacts of additives on performance and emission characteristics of diesel engines during steady state operation. Progress in Energy and Combustion Science 2017; 59: 32–78.

[4]. Nithya S, Manigandan S, Gunasekar P, Devipriya J, Saravanan WSR. The effect of engine emission on canola biodiesel blends with TiO_2. International Journal of Ambient Energy 2019; 40 (8): 838–41.

[5]. Venu H, Madhavan V. Effect of diethyl ether and Al_2O_3 nano additives in diesel-biodiesel-ethanol blends: Performance, combustion and emission characteristics. Journal of Mechanical Science and Technology 2017;31: 409–20.

[6]. Panda KJ, Sastry KRG, Rai NR. Experimental analysis of performance and emission on DI diesel engine fueled with diesel-palm kernel methyl ester-triacetin blends: a Taguchi fuzzy-based optimization. Environmental Science and Pollution Research 2018; 25: 22035-51.

[7]. Sudeshkumar PM, Joseph Raj Francis Xavier, Pandian Balu, Veerasundaram Jayaseelan, Kumarasamy Sudhakar. Waste plastic oil to fuel: An experimental study in thermal barrier coated CI engine with exhaust gas recirculation. Environmental Quality Management 2022; 32(1): 125-31.

[8]. Balu P, Vasanthkumar P, Govindan P, Sathish T. An experimental investigation on ceramic coating with retarded injection timing on diesel engine using Karanja oil methyl ester. International Journal of Ambient Energy 2023; 44(1): 1031-35.

[9]. Sabarish R, Prem Jeya Kumar M, Rajasekar R. Experimental investigation on direct injection diesel engine fuelled by JFO with nano additives. Materials Today: Proceedings 2022; 62 (4): 1821–29.

[10]. Harigaran A, Pandian Balu. An experimental study on the performance and emission characteristics of a single-cylinder diesel engine running on biodiesel made from palm oil and antioxidant additive. International Journal of Ambient Energy 2023; 44(1): 1076-80.

[11]. Sabarish R, Prem Jeya Kumar M. Experimental investigation of single cylinder DI diesel engine by diesel–JFO and its blends. AIP Conference Proceedings 2020; 2311(1) 020001 (2020).

[12]. Ramanujam Soundararaj, Joseph Raj Francis Xavier, Rajendiran Ramadoss, Pandian Balu, Veerasundaram Jayaseelan. Surface Ignition using ethanol on Mo and Al_2O_3 -TiO_2 coated in CI engine for environmental benefits. Advances in Environmental Technology 2021; 7(1): 19-27.

[13]. Sabarish R, Prem Jeya Kumar M. Experimental investigation of single cylinder DI diesel engine by diesel–JFO and its blends. AIP Conference Proceedings 2020; 2311(1) 020001 (2020).

[14]. Balu P, Saravanan P, Jayaseelan V. Effect of ceramic coating on the performance, emission and combustion characteristics of ethanol DI diesel engine. Material Today-Proceedings 2021; 39(4): 1259-64.

[15]. Prabu A, Anand RB. Emission control strategy by adding alumina and cerium oxide nano particle in biodiesel. Journal of the Energy Institute 2016; 89(3):366-72.

[16]. Ray S, Prakash O. Biodiesel Extracted from Waste Vegetable Oil as an Alternative Fuel for Diesel Engine: Performance Evaluation of Kirlosker 5 kW Engine. Renewable Energy and its Innovative Technologies 2018, Springer; 219-29.

[17]. Sakthivel Gnanasekaran, Saravanan N, Ilangkumaran M. Influence of injection timing on performance, emission and combustion characteristics of a DI diesel engine running on fish oil biodiesel. Energy 2016; 116(1): 1218-29.

[18]. Seraç RM, Aydın S, Yılmaz A, Şevik S. Evaluation of comparative combustion, performance, and emission of soybean-based alternative biodiesel fuel blends in a CI engine. Renewable Energy 2020; 148: 1065-73.

[19]. Golden Renjith Nimal RJ, Jacob S. Ensembles of Decision Rules to Predict Brake thermal efficiency of Bio Diesel with Nanoparticles. Knowledge Transactions on Applied Machine Learning 2023; 1(3): 18-29.